NATURAL CONVECTION WITHIN A LOOP WITH COLD-FLOW INJECTION

A. Skillen[1,*,†], R. Tunstall[2], S. Parry[2], S. Hind[2], S. Treasure[2]

[1]Department of Mechanical, Aerospace and Civil Engineering, University of Manchester, Manchester M13 9PL, United Kingdom
[2]Rolls-Royce, Kings Place, 90 York Way, LONDON, N1 9FX, United Kingdom

ABSTRACT

Large Eddy Simulation and unsteady RANS computations of flow around a natural convection loop have been performed. After reaching a statistically steady state, transient cold flow injection is introduced at the bottom of the loop for 2000 s before stopping. Depending upon the mass flow rate of this injection, the cold flow is observed to cause stall of the natural convection flow, or to diminish its flow rate, leading to a potential increase in heater temperature. This has important implications for the cooling of the primary loop of a reactor, where cold flow injection may be desirable under fault conditions. Interestingly, intermittent recovery of the NC flow is observed at the highest injection flow rate. The mechanism behind this recovery has been explored.

1 Introduction

Natural convection (NC) plays an important role in nuclear safety. For reactors relying on NC, their design ensures that coolant flow, driven by buoyancy, will be able to maintain sufficient heat transfer from the reactor core in the event of forced-convection pump failure. Of course, this requires extensive testing prior to accepting its viability for a given reactor design.

In addition to passive natural convection, it is often desirable under fault conditions to inject cold fluid into the primary loop to act as an additional coolant. However, the dynamics of cold-flow injection into a naturally circulating loop are poorly understood. Cold flow can lead to stall of the natural convection as stably stratified layers form, potentially leading to elevated reactor core temperatures over an initial transient. Such elevated temperatures need to be well understood and quantified to assess viability of a given design.

Numerically assessing the performance of the coolant under fault conditions is challenging. Buoyancy augments or suppresses local turbulence levels, while complex three-dimensional flow phenomena with stratification layers and flow recirculation is typical. In addition, flow injection is potentially subject to the well-known flow instabilities of a jet in cross flow [1], depending on the injection flow rate. These features are particularly challenging to accurately predict using 1D systems codes.

The aim of this study is twofold: 1) to assess the viability of URANS in predicting the dynamic response and subsequent recovery of single-phase natural convection flow subject to transient cold-flow injection. 2) To understand better the rich dynamics and flow-physics of this flow. These aims are supported by conducting high-fidelity wall resolved LES simulations at scale, which act as benchmark data for comparison. We focus on a relatively simple NC loop to facilitate investigations using high fidelity simulation, but it is expected that the loop exhibits the same key phenomena as found in real applications. It is also envisaged that the same NC loop will be studied experimentally using high-resolution and accurate measurements techniques in the future.

*Corresponding Author: alex.skillen@manchester.ac.uk
† Calculations performed while AS was at the Scientific Computing Department, The Science and Technology Facilities Council, Daresbury Laboratory, WA4 4AD

2 Methodology

2.1 Geometry

A sketch of the geometry of the loop is shown in Figure 1. The loop's height is 4 m (from pipe-centreline to centreline) at the tallest point, while the width (from centreline to centreline) is 2.5 m. The upper pipework has an angle of inclination of 5° to the horizontal. The three horizontal lengths of pipework forming the U-shaped bends are of equal length, while the centreline vertical distance between the upper and two lower horizontal lengths is 2.5 m. All the bends in this loop have a radius of curvature equal to one pipe diameter, while all the pipework comprising this loop has an internal diameter of 0.3 m.

The heated section of this loop starts 1 cm downstream of the neighbouring pipe bend (see Figure 1) and is 0.643 m in length. The start of the cooler is located 1 mm downstream of its neighbouring bend (see Figure 1) and is 0.667 m in length.

In addition to the loop pipework, the ability to inject fluid into the loop is facilitated through the addition of a T-junction connected to the central part of the right-hand horizontal pipework. This injection pipework has an internal diameter equal to $1/20^{th}$ that of the main loop. The injected fluid is allowed to exit through a surge connection with diameter equal to $1/10^{th}$ that of the main loop. The surge line forms a T-junction with the left vertical leg of the loop 2.5 m above the centreline of the lowest horizontal pipework legs. The surge exit is at the same height as the top of the loop, while the bend along the surge connection has radius equal to one diameter of the main loop pipework. The horizontal pipework along the surge connection is 0.33 m in length.

2.2 Boundary and volumetric conditions

The heated section is modelled as a uniform volumetric heat source with 25kW heat output. The cooler is modelled through conjugate heat transfer which enforces consistency of the heat flux and temperature at the interface between solid and fluid domains:

$$T_s = T_f \qquad \kappa_s \left(\frac{\partial T}{\partial n}\right)_s = \kappa_f \left(\frac{\partial T}{\partial n}\right)_f$$

where where subscripts $(\cdot)_f$ and $(\cdot)_s$ denote the fluid and solid domains, respectively, κ is the thermal conductivity, and n is the outward-pointing interface-normal. The cooler wall is 1cm thick and is made of copper (density: 8940 kg/m3, thermal conductivity: 398 W / m / K, specific heat capacity: 385 J / Kg / K). The external vertical wall of the cooler has a Dirichlet condition applied for the temperature, with a uniform value of 10C. All other walls are treated as adiabatic, with no-slip conditions applied.

Cold-flow injection is set to have uniform inlet boundary temperature of 5C. The mass flow rate of the injection is a parameter that varies in this study in the range [0.05 kg/s – 0.2 kg/s]. The cold injection commences at time $t = 0s$. Prior to this time, the flow is initialised to a statistically steady state. Between $t = 0$ s and $t = 1$s, the injection follows a linear ramp up to its final flow rate where it is held until $t = 2000$s. Between $t = 2000$ s and $t = 2001$ s the injection follows a linear ramp back down to 0 m/s as recovery commences.

Head losses with K=6.83 are applied at the heater, cooler and top-horizontal pipework (at the top of the u-bend) to mimic the effects of the heater cooler and additional losses in a real system. For the heater, this loss is distributed over the whole heated section. For the cooler, the loss is distributed over a 1cm length of pipework starting at the entrance to the cooler. The additional loss is distributed over a 1cm length of pipework starting at the intersection between the exit of the bend and start of the horizontal pipework at the top of the U-Bend. This configuration was chosen to closely match conditions that will be applied to a future planned experimental rig.

2.3 Governing Equations Computational meshes and Discretisation

Unsteady RANS computations employ meshes of around 30M computational cells. LES computations are discretised with approximately 150M computational cells. In both cases, the meshes are generated through a hybrid strategy in which most of the computational domain is discretised with block-structured hexahedral cells. The exception to this localised to the T-junctions where the inlet and surge connections join onto the main loop. These T-junctions are particularly challenging to mesh through standard block-structured approaches due to the large diameter ratio between the main pipework and the auxiliary pipes. We therefore applied localised unstructured meshes with a hexahedral dominant octree mesh which is "snapped" to conform to the geometry.

The flow is governed by the dilatable Navier-Stokes equations which have been either filtered (in the case of LES) or Reynolds averaged (in the case of URANS). In both cases, the governing equations are discretised through the finite volume method and are solved with second order accuracy in both time and space. Central schemes are employed for the LES, while 2nd order upwind schemes are employed for the URANS computations. Our URANS results are closed using the EBSRM model with a GGDH model for turbulent heat fluxes [2,3]. All LES results closed through a dynamic Smagorinsky model. All fluid properties are allowed to vary with temperature, following a 6th order polynomial fitted to water properties.

3 Results

Figure 2 shows temperature contours from the LES with a 0.2 kg/s injection at time 250 s (towards the start of the transient). Stratified layers are observed on the cold leg as the cold-flow injection impinges onto the upper wall of the pipe, supressing the NC flow. In Figure 3, the evolution of loop mass flow rate is presented. The temperature difference between the heater and cooler is presented in Figure 4.

The URANS is predicting broadly the same dynamic response to that of the LES, except for intermittent periods of natural convection recovery at the highest injection rate which are observed in the LES, but not predicted by URANS. To investigate this further, we plot temperature contours in Figure 5, showing the evolution of the transient. We focus in particular on the second intermittent recovery, the onset of which occurs at $t \approx 615$ s before returning to a deep stalled state by $t \approx 1045$ s (see Figure 3). In Figure 5a, we observe a stably stratified layer forming on the bottom of the cold leg. This stable stratification causes the stall of the NC flow. Between $t = 395$ s and $t = 515$ s (Figure 5a and Figure 5b, respectively), prior to the onset of the intermittent recovery, two things of significance are observed: 1) the cold flow injection starts to "fill" the left-vertical section of the right U-bend, and 2) the stalled flow around the cooler drops significantly in temperature due to the low mass flow rate due to stall. This drop in cooler temperature causes the rise in ΔT between the heater and cooler at approximately $300\ s < t < 615$ s.

By $t \approx 615$ s, the cold flow "filling" the left leg of the U-bend starts to spill over the top of the U (Figure 5c). This cold flow sinks down the right-leg of the left U-bend due to buoyancy forces, causing the onset of the second intermittent recovery in the NC flow (note the start of the 2nd recovery observed in Figure 3 occurs at $t \approx 615$ s, corresponding to the state in Figure 5c). This leads to a pick-up of the loop flow rate, convecting warmer fluid through the cooler, in turn leading to a reduction in ΔT between the heater and cooler. Note that the peak in ΔT at $t \approx 615$ s in Figure 4 corresponds with the onset of the NC recovery in Figure 3, also at $t \approx 615$ s.

By $t \approx 815$ s, the intermittent recovery reaches a (local) peak flow rate (Figure 3). This corresponds to the state shown in Figure 5d. In this figure, we can see that the left U-bend is starting to cool, reducing the effect of the buoyancy driven recovery as cold flow spills over the top of the U-bend. At $t \approx 1045$ s, the intermittent recovery is finalised, and a deep stall is again observed (characterised by low flow rates in Figure 3, only just above the injection flow rate). Stable stratification on the bottom of the cold

leg is again observed, similar to in Figure 5a, but at a lower overall temperature. This cycle repeats a few hundred seconds later.

In our URANS computations, the above mechanism is not well predicted. The main source of discrepancy appears to be related to the dynamics of the overspill from the top of the U-bend. In the LES, the cold fluid separates from the wall, leading to strong buoyancy forces as the cold fluid is located towards the centre of the pipe. In our URANS predictions (see Figure 6), contrary to the LES, the cold fluid remains attached to the wall where buoyancy forces are countered by viscous forces from the no-slip condition. The source of this discrepancy warrants further investigation, but it is worth noting that the URANS prediction is a conservative one, which gives us some confidence in its use under design conditions.

Recovery of the NC after turning off the injection is delayed, with no sign of recovery in the 1000s following the injection stopping for URANS at the highest injection rate.

4 Conclusions

High-fidelity simulations of flow around a NC loop with cold flow injection have been performed. We observe interesting flow dynamics, particularly at higher injection flow rates. Intermittent recovery of the NC is linked to cold flow over the top of the U-Bend. URANS fails to predict this intermittency due to the flow remaining attached to the wall, significantly altering the local buoyancy force.

Three different injection flow rates have been investigated. In all cases, the URANS predictions are both satisfactory and conservative (i.e. predicting lower flow rates and slightly higher temperatures than in the LES).

Our future work in this area will explore in greater detail the flow physics of the lower flow injection rates (which were only briefly discussed here due to the imposed page limit).

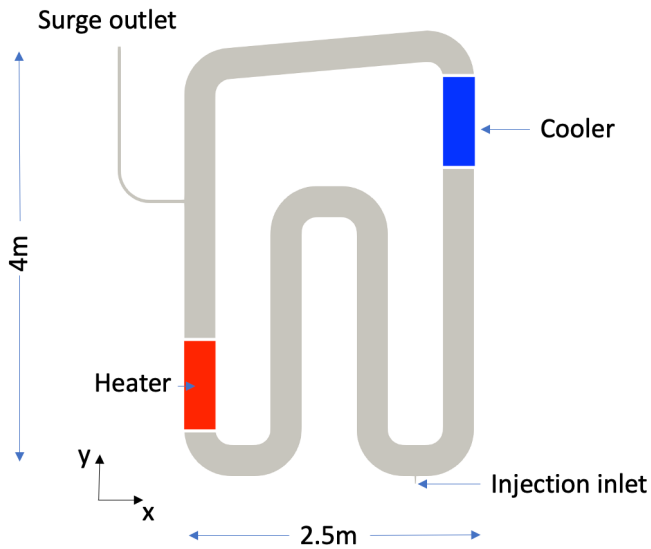

Figure 1: Loop geometry.

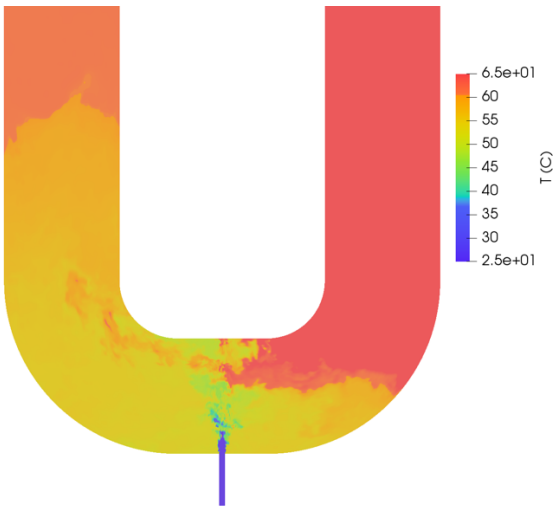

Figure 2: Close up around injection for $\dot{m}_{inj} = 0.2$ kg/s at t=250 s, showing LES predicted temperature on symmetry plane.

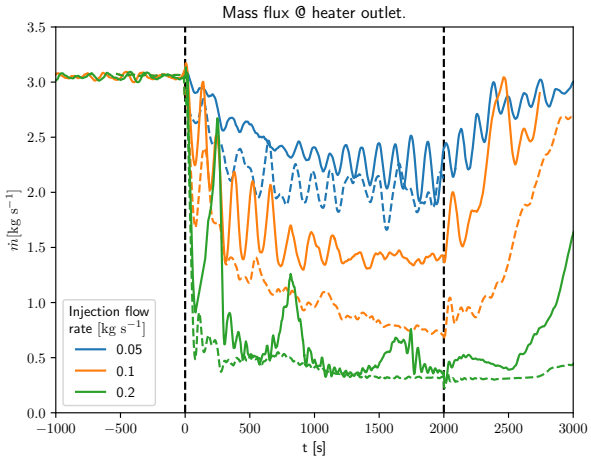

Figure 3: Mass flow rate through heated section. Solid lines are LES computations, while dashed lines are URANS results. Vertical dashed lines indicate start and end of injection. Colours indicate injection flow rate.

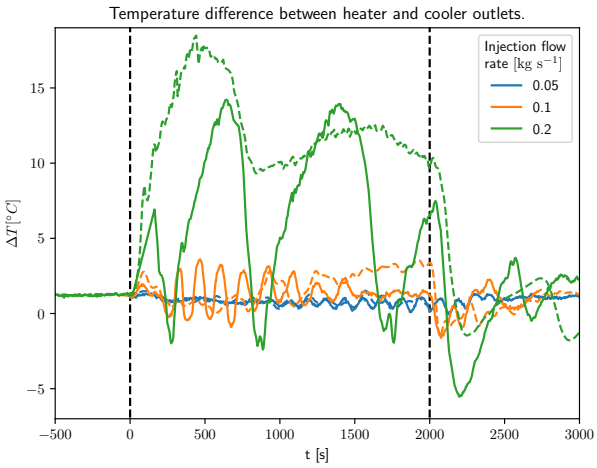

Figure 4: Temperature difference between heater and cooler outlets. Solid lines are LES computations, while dashed lines are URANS results. Vertical dashed lines indicate start and end of injection. Colours indicate injection flow rate.

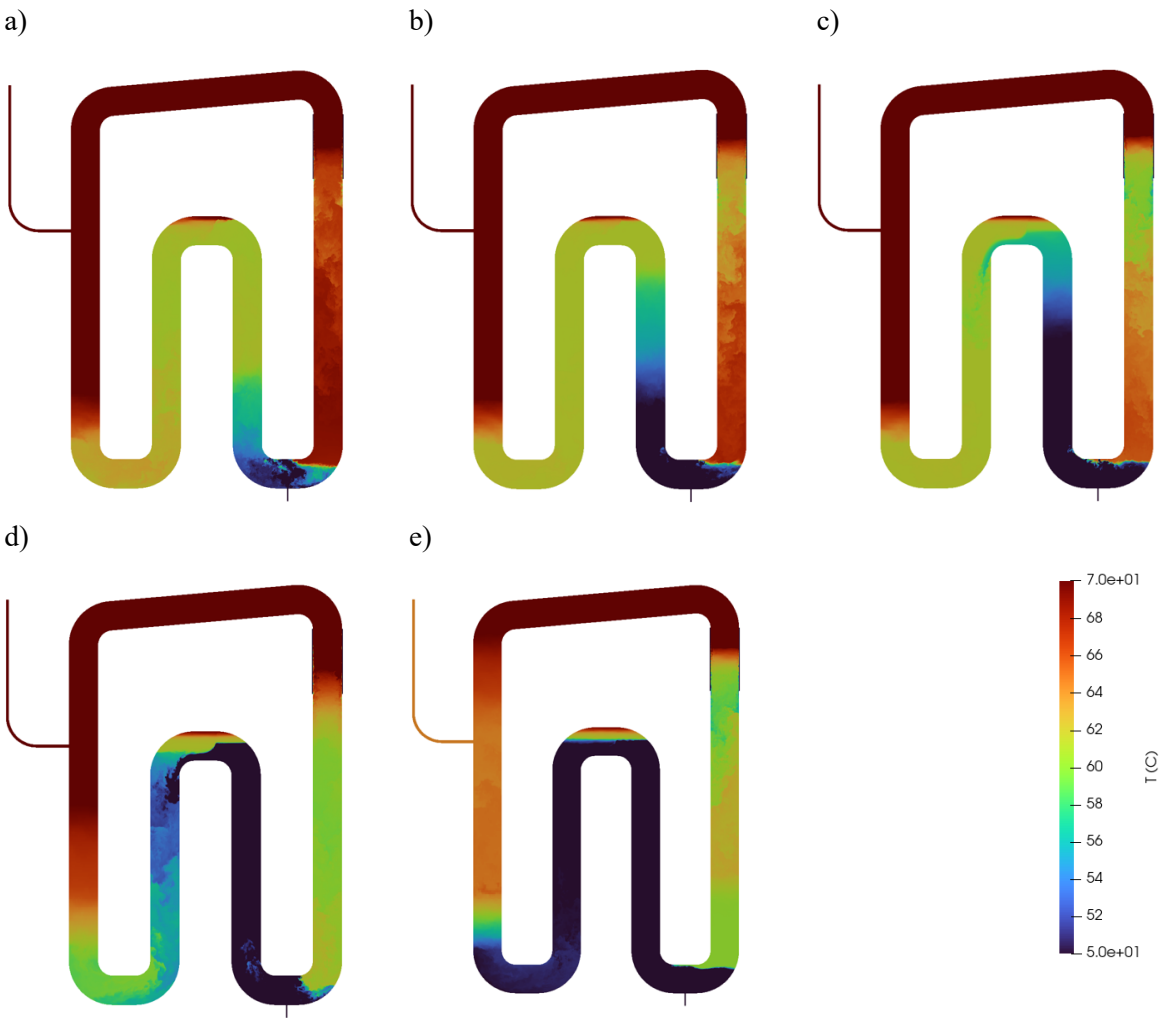

Figure 5: Contours of temperature on the symmetry plane showing evolution of transient for $\dot{m}_{inj} = 0.2$ kg/s at: a) t=395 s. b) t=515 s. c) t=615 s. d) t=815 s. e) t=1045 s. LES predictions.

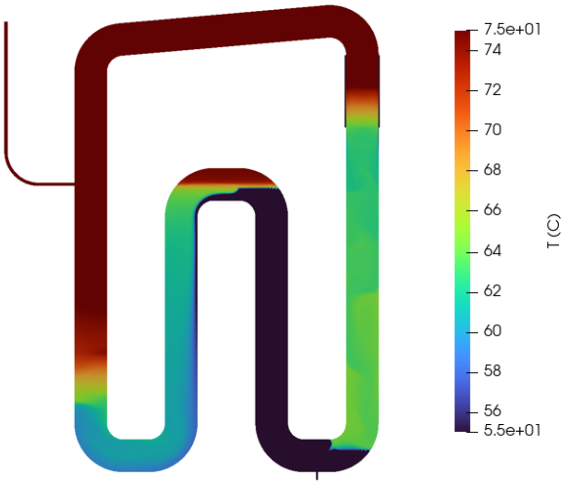

Figure 6: URANS temperature contours on the symmetry plane for $\dot{m}_{inj} = 0.2$ kg/s, at time $t = 815\ s$.

ACKNOWLEDGEMENTS

The authors would like to thank EPSRC for the computational time made available on the UK supercomputing facility ARCHER2 via the UK Turbulence Consortium ***(EP/R029326/1)***

REFERENCES

[1] Kamotani, Y. and Greber, I., 1972. Experiments on a turbulent jet in a cross flow. *AIAA journal*, *10*(11), pp.1425-1429.

[2] Manceau, R. and Hanjalić, K., 2002. Elliptic blending model: A new near-wall Reynolds-stress turbulence closure. *Physics of Fluids*, *14*(2), pp.744-754.

[3] Daly, B.J. and Harlow, F.H., 1970. Transport equations in turbulence. *The physics of fluids*, *13*(11), pp.2634-2649.